

RSC Advances



This is an *Accepted Manuscript*, which has been through the Royal Society of Chemistry peer review process and has been accepted for publication.

Accepted Manuscripts are published online shortly after acceptance, before technical editing, formatting and proof reading. Using this free service, authors can make their results available to the community, in citable form, before we publish the edited article. This *Accepted Manuscript* will be replaced by the edited, formatted and paginated article as soon as this is available.

You can find more information about *Accepted Manuscripts* in the [Information for Authors](#).

Please note that technical editing may introduce minor changes to the text and/or graphics, which may alter content. The journal's standard [Terms & Conditions](#) and the [Ethical guidelines](#) still apply. In no event shall the Royal Society of Chemistry be held responsible for any errors or omissions in this *Accepted Manuscript* or any consequences arising from the use of any information it contains.

ARTICLE

New Understanding on the Reaction Pathways of the Polyacrylonitrile Copolymer Fiber Pre-Oxidation: Online Tracking by Two-Dimensional Correlation FTIR Spectroscopy

Cite this: DOI: 10.1039/x0xx00000x

Received 00th January 2012,
Accepted 00th January 2012

DOI: 10.1039/x0xx00000x

www.rsc.org/

Jing Zhao, Jihai Zhang, Tao Zhou,* Xifei Liu, Qiang Yuan, and Aiming Zhang

Polyacrylonitrile (PAN) copolymer fiber pre-oxidation has an important influence on the final properties of carbon fibers. Understanding and tracking the reaction pathways of the pre-oxidation has a great significance for guarantee the quality of the resulting carbon fibers. In this study, the *in situ* FTIR spectroscopy combining the scaling moving-window two-dimensional correlation spectroscopy (scaling-MW2D) and 2D correlation analysis were used to study the reaction pathways. In addition, DSC and ^{13}C solid-state NMR were used to assist the determination and to verify the chemical structure. Scaling-MW2D revealed that the pre-oxidation consisted of the initial process (A, 69–223 °C) and the main process (B, 223–309 °C). From the sequential order of 2D correlation analysis, the more detailed pathways were obtained. The induced reaction of comonomer units took place in process A (69–223 °C). In process B (223–309 °C), the initial cyclic structures were first generated from the induced structure formed in process A. Then, these initial cyclic structures underwent a series of the oxidation, the subsequent isomerization, and so on. After that, a large number of AN units were immediately involved in the main cyclization reaction, and some of β -amino nitriles was produced. One of new understandings obtained was that the initial cyclic structures after the oxidation, the isomerization, and so on were the real induced “nucleus” of the main cyclization reaction, and therefore, the oxygen in the air played a key role on the PAN main cyclization. The last step was the dehydrogenation reaction on the polycyclic structures at high temperature.

1. Introduction

Carbon fibers are an excellent material with ultrahigh mechanical strength, superior corrosion-resistant, lightweight, and it has been widely applied in the automotive, civilian industry, sports apparatus, especially in the field of aerospace.^{1–3} It's worth mentioning that polyacrylonitrile (PAN) precursor fiber is one of the most popular raw materials for producing high performance carbon fibers.^{4–8} Generally speaking, the mainly manufacturing process of PAN-based carbon fibers involves pre-oxidation and carbonization, in which pre-oxidation is a complex and time-consuming process. The typical pre-oxidation procedure of PAN precursor fibers are calcined at 200–300 °C in the tube furnace for 1–2 h.^{8–10} Pre-oxidation process has an important influence on the final properties of carbon fibers. Therefore, understanding and tracking the pre-oxidation reaction pathways has a great

significance for guarantee the quality of the resulting carbon fibers and improves production efficiency.

Many researchers^{11, 12} found that a series of chemical reactions occurred during the pre-oxidation process of PAN, primarily including cyclization, dehydrogenation, oxidation, and so on. It was verified that the qualities of pre-oxidation are strongly depended on the experimental conditions, such as the atmosphere, time, temperature, oxygen diffusion. To date, the pre-oxidation mechanism of PAN have been intense investigations with various methods, such as solid-state nuclear magnetic resonance (ssNMR),^{1, 10, 13, 14} Fourier transform infrared spectroscopy (FTIR),^{10, 13, 15–17} elemental analysis,¹⁸ thermal analysis,¹⁹ X-ray diffraction.¹⁹ According to the literature, Ngoc Uyen et al.¹⁵ investigated the structural evolution of poly(acrylonitrile-coitaconic acid) (PAI) by FTIR during the pre-oxidative, and determined the optimal structural characteristics of the precursors for carbon fibers. Liu et al.⁵ systematically studied the thermo-chemical reactions and the

structural conversions of the electrospun PAN precursor nanofibers during the pre-oxidative. It was revealed that the PAN copolymer predominantly participates into the intermolecular cyclization or crosslinking. They also compared the electrospun PAN nanofibers with the conventional precursor fibers (SAF 3K) produced by wet spinning. Wang et al.¹ analyzed the composition and structure of the residues after the thermal treatment of ¹³C-labeled PAN samples in the argon atmosphere by one and two-dimensional solid-state ¹³C nuclear magnetic resonance (ssNMR) experiments. Very recently, Liu et al. systematically investigated the ¹³C-labeled a-PAN stabilized different reaction pathways and structures under nitrogen and air atmosphere using several ss-NMR techniques.¹⁹ Despite decades of research, however, the proposed reaction pathway (or mechanism) of this process is still puzzling.^{1, 11, 20} Moreover, most current investigations based on the pre-oxidized PAN fibers are non-online, and strongly depending on the environmental factors.²¹⁻²³ Therefore, the precise online tracking the reaction pathways of the pre-oxidation process of PAN fibers will be urgent and of great importance. Herein, we proposed an online approach to track this process using two-dimensional (2D) correlation FTIR spectroscopy.

Generalized two-dimensional (2D) correlation infrared spectroscopy was originally proposed by Noda in 1993.²⁴ This technique is one of the best ways to study polymer transition mechanism, which can be easily used to track chemical structure information by the sequential order of spectral variables. In 2000, in order to identify the transition temperature of a thermotropic liquid-crystal sample, the theory of the moving-window two-dimensional correlation spectroscopy (MW2D) was reported by Thomas and Richardson.²⁵ After that, a similar technique based on the MW2D was proposed by Morita in 2006, called perturbation-correlation moving-window two-dimensional correlation spectroscopy (PCMW2D).²⁶ One of the biggest advantages is that MW2D can be directly used to determine the spectral correlation variation along both perturbation variables (e.g., temperature) and spectral variables (e.g., wavenumber) axis.²⁶⁻³⁰ Recently, we have proposed the scaling moving-window two-dimensional correlation spectroscopy (scaling-MW2D), which was specially designed to identify weak transitions of polymers.³¹ The reason of establishing scaling-MW2D is that the conventional MW2D has a difficulty to distinguish the weak transitions due to its low resolving capacity along the perturbation variable axis (e.g., temperature).³¹ The 2D correlation infrared spectroscopy has an inherent advantage in the study of polymer transitions. In recent years, the combination of 2D correlation infrared spectroscopy with moving-window and generalized 2D correlation analysis has been widely applied to investigate the glass transition, the reaction mechanism, the crystallization temperature, and other phase-transitions of polymers, which was proven to be very convenient and successful.³²⁻³⁶ Hence, 2D correlation FTIR spectroscopy is also suitable for PAN fibers to online monitor

the pre-oxidation process, as well as to study the reaction pathways.

In the present study, the *in situ* FTIR spectroscopy combining scaling-MW2D and 2D correlation analysis were employed to investigate the reaction mechanism of the pre-oxidation. Scaling-MW2D revealed that the pre-oxidation reaction of PAN copolymer fibers had two processes, called process A (69–223 °C) and process B (223–309 °C). An accurate and systematic reaction route was obtained. Furthermore, the differential scanning calorimeter (DSC) was also used to assist the determination of the temperature region and solid-state ¹³C NMR analysis was applied to verify the molecular structure of pre-oxidized PAN fibers.

2. Experimental

2.1. Materials

Polyacrylonitrile (PAN) copolymer fibers (methyl acrylate as the co-monomer with 1.0 mol%; the average diameter was 5 μm) which was prepared via dry-wet spinning, were provided by Zhejiang Zhongcheng Packing Material Co., Ltd. The weight average molecular weight (M_w) was 1.34×10^6 g/mol measured by gel permeation chromatography (GPC). The GPC results of PAN copolymer fibers are listed in **Table S1** in the supporting information. The PAN samples were used as received without any further treatment.

2.2. Differential scanning calorimetry (DSC)

The DSC measurement was performed on NETZSCH 204 F1 with 8 mg of PAN fibers sample in air atmosphere (25 mL/min). The sample was heated from 50 °C to 320 °C at 5 °C/min.

2.3. Thermal gravimetric analysis (TGA)

The thermogravimetric behavior was measured using a NETZSCHTG 209F1 thermal gravimetric analyzer at a heating rate of 5 °C/min in the range of 40–600 °C in air atmosphere (25 mL/min). The sample weight of PAN fibers was 5 mg.

2.4. *In situ* FTIR spectroscopy

The PAN fibers were firstly cut into powder, and then ground approximately 5 mg of this powder with 300 mg KBr until the fiber powder was uniformly dispersed. After desiccated, the mixed powder was tableted to a disk with the diameter of 1.3 cm and the thickness of 0.8 mm. The temperature-dependent FTIR spectra between 60 °C and 320 °C were collected with Nicolet iS50 Fourier transform spectrometer, which was equipped with a deuterated triglycine sulfate (DTGS) detector. The FTIR spectra of the sample were recorded within the region of 4000–400 cm^{-1} at a resolution of 4 cm^{-1} with 32 scans. The temperature-dependent FTIR experiment was carried out in air atmosphere and the heating rate was 5 °C/min. A total of 122 FTIR spectra were gathered from 60 °C to 320 °C at approximately 2 °C increments.

2.5. 2D correlation analysis

The generalized 2D correlation FTIR spectra, MW2D, and scaling-MW2D were processed, calculated, and plotted by 2DCS software, developed by one of the authors. The window size of MW2D and scaling-MW2D was chosen as 11 (2m+1) to produce high-quality spectra. The linear baseline corrections were applied in the region of 3470–2750 cm^{-1} , 2400–2100 cm^{-1} , and 1780–840 cm^{-1} before the calculations. The 5% correlation intensity of spectra was regarded as noise and was cut off. In 2D correlation FTIR spectra, the red areas represent positive correlation intensity, and the blue areas represent the negative correlation intensity. The theory and algorithm of MW2D and generalized 2D correlation spectroscopy can refer to the literature.^{24, 25} A brief summarization to the theory of scaling-MW2D based on auto-correlation is described in the supporting information. The detailed algorithm of scaling-MW2D can also refer to the Ref.³¹

2.6. Solid-state ^{13}C NMR and ^1H NMR

The pre-oxidized PAN copolymer fibers were prepared using SK-G10123K furnace (Tianjin Central laboratory furnace Ltd.). The PAN fibers were kept straight and program temperature heated from 60 $^{\circ}\text{C}$ to 320 $^{\circ}\text{C}$ at 5 $^{\circ}\text{C}/\text{min}$ with the air flow rate of 1.5 L/h. After that, both the raw PAN fibers and the pre-oxidized PAN fibers were cut into powder. The ^{13}C solid-state NMR (^{13}C ss NMR) of the powders of PAN fibers and pre-oxidized PAN fibers were measured using a Bruker Avance Ultrashield 500 Plus NMR. The ^1H and ^{13}C carrier frequencies were 500.1 and 125.8 MHz, respectively. In this study, the parameters of ^{13}C ss NMR measurements were chosen as the report by Liu et al.¹⁹ The as-prepared samples were packed in a 4 mm Zirconia MAS rotor with a Kek-F drive cap and were measured with a MAS speed of 13 kHz at 25 $^{\circ}\text{C}$. The CH signal was set as 29.46 ppm as an external reference. In ^{13}C CP/MAS experiments, ^{13}C 90 $^{\circ}$ pulse length, CP contact time, and recycle delay were set as 2.5 μs , 5 ms, and 2 s, respectively. The ^1H NMR of PAN copolymer fibers was also measured using a Bruker Avance 600 MHz NMR spectrometer, and the deuterated dimethyl sulfoxide (DMSO- d_6) was used as the solvent. The ^1H NMR of PAN fibers is shown in Figure S1 in the supporting information.

3. Results and discussion

3.1. Structure evolution of PAN copolymer fibers upon heating

The *in situ* FTIR spectra of PAN copolymer fibers upon heating from 60 $^{\circ}\text{C}$ to 320 $^{\circ}\text{C}$ in the region 3450–2740 cm^{-1} , 2280–2120 cm^{-1} , and 1850–850 cm^{-1} are shown in Figure 1. According to the literature, the bands assignments in this paper are summarized in Table S2 in the supporting information. The peak at 1733 cm^{-1} is assigned to C=O stretching of methyl methacrylate (MMA).^{8, 15} It can be observed the intensity of 1733 cm^{-1} reduces with the temperature increasing. This indicates the disappearance of MMA repeating units during the pre-oxidation process. Commonly, the most representative spectral region for PAN fibers is 2280–2120 cm^{-1} , because the

peak at 2243 cm^{-1} assigned to C \equiv N stretching.^{10, 13, 15, 17} As the temperature increases from 60 $^{\circ}\text{C}$ to 320 $^{\circ}\text{C}$, the bands intensity of nitrile grouping (2243 cm^{-1}) rapidly reduces, and slightly moves to a lower wavenumber (about 10 cm^{-1}). The bands intensity decrease of 2243 cm^{-1} certainly reveals the disappearance of ordinary C \equiv N groups during the pre-oxidation, and the phenomenon of moving to a lower wavenumber was reported due to the electron resonance of nitrile grouping with other groups in molecular chains.³⁷ It is noted that the peak around 2243 cm^{-1} does not completely disappear at 320 $^{\circ}\text{C}$,

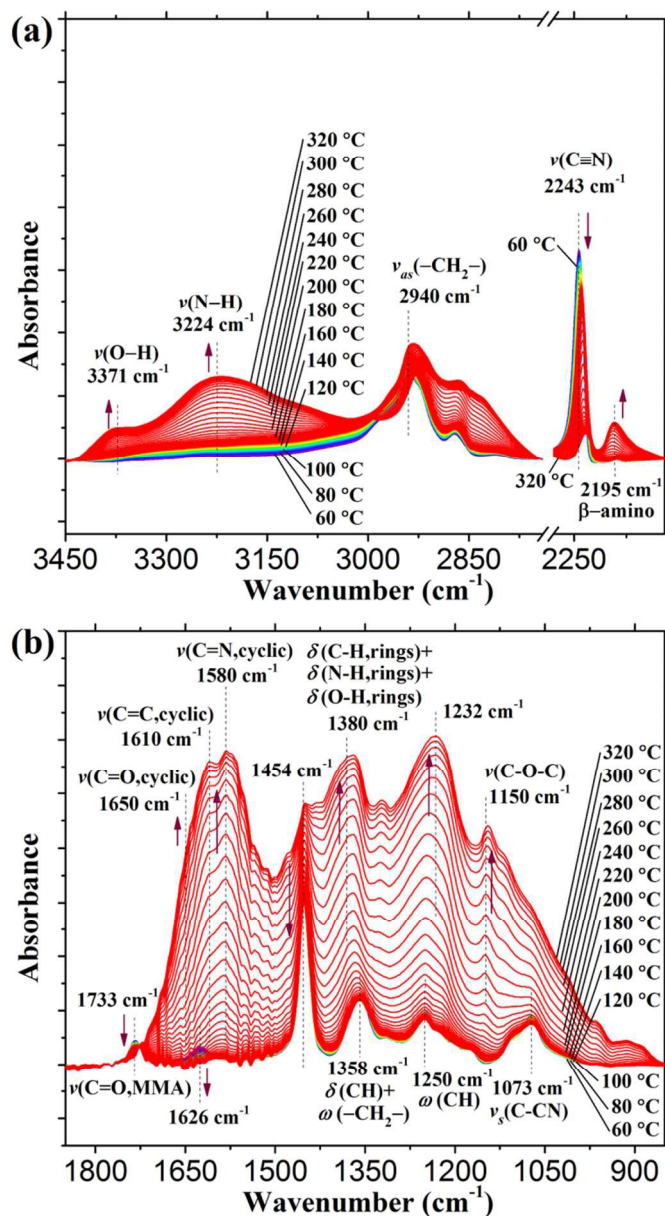


Figure 1. *In situ* FTIR spectra of the pre-oxidation of PAN copolymer fibers from 60 $^{\circ}\text{C}$ to 320 $^{\circ}\text{C}$. Key: (a) 3450–2740 cm^{-1} and 2280–2120 cm^{-1} ; (b) 1850–850 cm^{-1} .

which indicates the not all of the nitrile grouping in PAN fibers can be converted into a ladder-like polymer structure during the pre-oxidation process. There still exists the residual isolated nitrile in the molecular chains after the pre-oxidation. In

addition, a new peak is observed around 2195 cm^{-1} which was also reported by Satish et al.³⁸ They deconvoluted the overlapping bands within 2250–2150 cm^{-1} using multi-peak fitting, and two peaks of 2190 cm^{-1} and 2210 cm^{-1} were successfully fitted, which are assigned to $\text{C}\equiv\text{N}$ stretching of $\text{C}\equiv\text{N}$ groups in β -amino nitrile and conjugated nitrile,^{38, 39} respectively. The appearance of 2195 cm^{-1} reveals the transformation from the ordinary $\text{C}\equiv\text{N}$ groups to β -amino nitrile during the pre-oxidation.

At the same time, it is also observed that the bands intensities of 3371 cm^{-1} and 3224 cm^{-1} which are assigned to O–H stretching of O–H groups and N–H stretching of N–H groups obviously increase from 60 $^{\circ}\text{C}$ to 320 $^{\circ}\text{C}$,^{15, 40, 41} indicating the generation of O–H and N–H groups. As shown in **Figure 1(b)**, most of the peaks in the region 1850–850 cm^{-1} suddenly rapidly widen and heighten with the temperature increasing. Special attention is needed to the new generated bands of 1610 cm^{-1} , 1580 cm^{-1} , and 1380 cm^{-1} . The bands of 1610 cm^{-1} , 1580 cm^{-1} are attributed to $\text{C}=\text{C}$ and $\text{C}=\text{N}$ stretching in the cyclic structure,^{42, 43} and 1380 cm^{-1} is an overlapped bands consisting of C–H, N–H, and O–H bending in rings.^{15, 43} This fully shows that a large number of cyclic structures generates during the pre-oxidation. In addition, the formation of the acridone and C–O–C structure is also detected, because the band intensity of 1650 cm^{-1} assigned to $\text{C}=\text{O}$ stretching of carbonyl groups in acridone^{42, 43} and that of 1150 cm^{-1} assigned to C–O–C stretching^{15, 44} both increase rapidly during the pre-oxidation. It is noted that the bands intensity around 2940 cm^{-1} rapidly decreases when the temperature is near 320 $^{\circ}\text{C}$. The peak around 2940 cm^{-1} is assigned to C–H asymmetrical stretching of $-\text{CH}_2-$ groups in PAN backbone, and therefore, the reduction of 2940 cm^{-1} probably reveals the occurrence of dehydrogenation reactions at the high temperature.

Table 1. ^{13}C resonances of raw PAN copolymer fibers and pre-oxidized PAN copolymer fibers observed in the ssNMR spectra.

	^{13}C chemical shifts (ppm)	Assignments	References
a	28.4	–CH–	1, 10, 20, 22
b	28.4	–CH ₂ –	1, 10, 20, 22
c	69.7	–C–OH	1, 20, 22
d	72.6	C–O–C	45, 46
e	112.8	–C=C–	13, 22
f	119.6	–C≡N	1, 10, 13, 22
g	134.3	–C=C–H	13, 22
h	145.6	–C=C–O	47
i	150.2	–C=N–	1, 20
j	162.4	O=C=N–	1, 20
k	164.0	C=C–NH ₂	39
l	196.4	–C=O	20

3.2. ^{13}C ssNMR

To further reveal the final chemical structure of pre-oxidized PAN copolymer fibers. Typical solid-state ^{13}C NMR spectra of raw PAN copolymer fibers and pre-oxidized PAN copolymer are measured and illustrated in **Figure 2**. The corresponding chemical structures are summarized in **Table 1**. The chemical shift at 119.6 ppm (f) is attributed to the $\text{C}\equiv\text{N}$ groups, and an

obvious reduction of 119.6 ppm confirms most of PAN fibers are involved in the pre-oxidation process.¹⁹

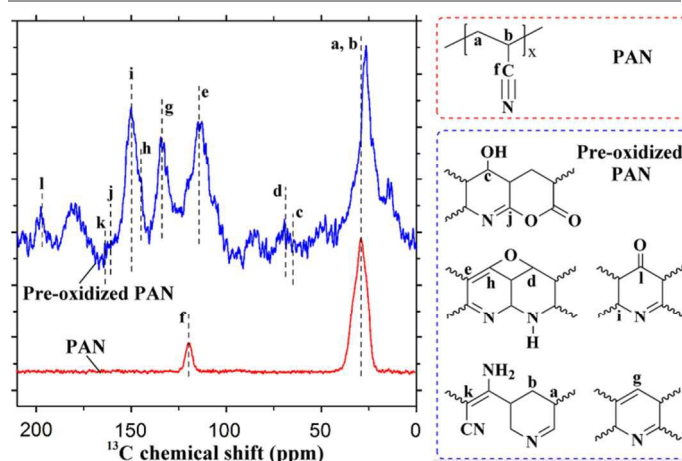


Figure 2. Solid-state ^{13}C NMR spectra of PAN copolymer fibers (red curve) and pre-oxidized copolymer PAN fibers (blue curve).

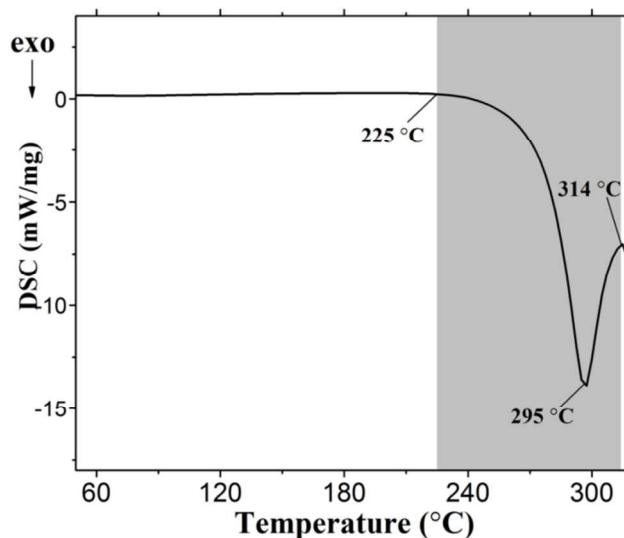


Figure 3. DSC curve of PAN copolymer fibers from 50 $^{\circ}\text{C}$ to 320 $^{\circ}\text{C}$ upon heating at 5 $^{\circ}\text{C}/\text{min}$ in air atmosphere.

Compared with the raw PAN fiber, there appears a series of new peaks in ^{13}C ssNMR spectra of pre-oxidized PAN fiber. Specifically, the appearances of 112.8 ppm (e), 134.3 ppm (g), 150.2 ppm (i), 145.6 ppm (h), 72.6 ppm (d), 196.4 ppm (l), 164.0 ppm (k), and 69.7 ppm (c) are observed. The chemical shifts at 112.8 ppm (e) and 134.3 ppm (g) are contributed from carbon atoms in $-\text{C}=\text{C}-$ and $-\text{C}=\text{C}-\text{H}$ structures, and 150.2 ppm (i) is assigned to the $-\text{C}=\text{N}-$ structure. The appearance of 112.8 ppm (e), 134.3 ppm (g), and 150.2 ppm (i) reveals the cyclization and dehydrogenation reactions, which is also detected in *in situ* FTIR in **Figure 1**. The chemical shift at 196.4 ppm (l) is attributed to $-\text{C}=\text{O}$ from pre-oxidation products while 145.6 ppm (h) and 72.6 ppm (d) are both attributed to C–O–C groups. Moreover, the chemical shifts at 164.0 ppm (k) and 69.7 ppm (c) are assigned to $\text{C}=\text{C}-\text{NH}_2$ and $-\text{C}-\text{OH}$ in the cyclic structures, respectively. Combining with

the results of *in situ* FTIR and ^{13}C ssNMR, the final chemical structure of the pre-oxidized PAN fibers can be clearly determined as shown in **Figure 2**. It also can be concluded that the pre-oxidation of PAN copolymer fibers primarily consists of cyclization, dehydrogenation, and the oxidation reaction. However, the specific reaction pathways based upon these results are still unclear. Therefore, the powerful 2D correlation FTIR spectroscopy is necessary for figuring out the reaction mechanism of the pre-oxidation of PAN copolymer fibers.

3.3. DSC measurement

DSC curve of PAN fibers from 50 °C to 320 °C upon heating in air atmosphere is measured and illustrated in **Figure 3**. An exothermic peak at 295 °C is observed, and the temperature range of this peak is within 225–314 °C, which is consistent with the range determined by TGA measurement (**Figure S2** in the supporting information). This indicates that pre-oxidation reaction of PAN fibers begins at 225 °C and ends at 314 °C, and this reaction reaches the maximum reaction rate at 295 °C. It is noted that no other peaks are observed when the temperature is below 225 °C.

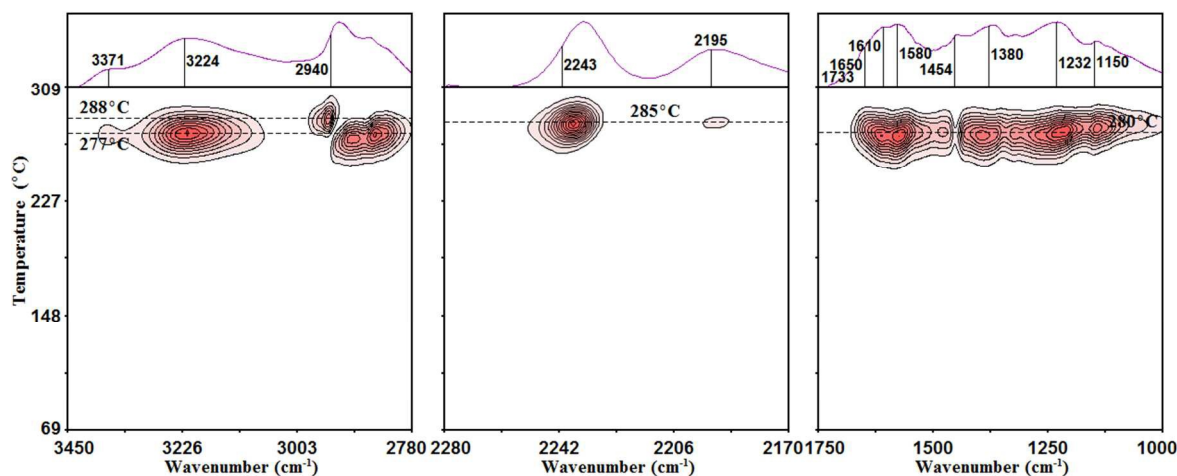


Figure 4. Conventional MW2D FTIR spectra of the pre-oxidation of PAN copolymer fibers calculated from the *in situ* FTIR spectra from 60 °C to 320 °C in the region of 3450–2780 cm^{-1} , 2280–2170 cm^{-1} and 1750–1000 cm^{-1} . The horizontal dashed lines correspond to the temperature points at 277 °C, 280 °C, 285 °C, and 288 °C.

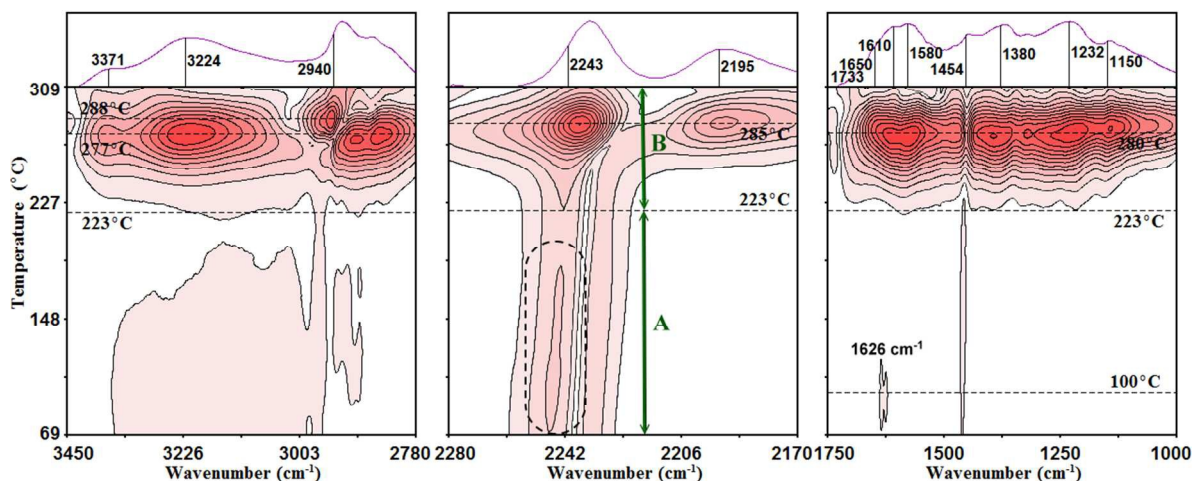


Figure 5. Scaling-MW2D FTIR spectra of the pre-oxidation of PAN copolymer fibers calculated from the *in situ* FTIR spectra from 60 °C to 320 °C in the region of 3450–2780 cm^{-1} , 2280–2170 cm^{-1} and 1750–1000 cm^{-1} . The scaling factor is chosen as $\alpha=0.7$. The horizontal dashed lines correspond to the temperature points at 100 °C, 223 °C, 277 °C, 280 °C, 285 °C, and 288 °C, respectively.

3.4. Two processes of pre-oxidation determined by scaling-MW2D FTIR

Figure 4 is the conventional MW2D FTIR spectra of the pre-oxidation of PAN copolymer fibers in the region of 3450–2780 cm^{-1} , 2280–2170 cm^{-1} and 1750–1000 cm^{-1} , which are calculated from the *in situ* FTIR spectra from 60 °C to

320 °C. A strong transition within 277–288 °C is observed. The temperature of 277–288 °C just falls into the temperature region of pre-oxidation reaction determined by DSC (225–314 °C). Thus, the transition within 277–288 °C observed in the conventional MW2D also reveals the pre-oxidation reaction. Specifically, temperature points at 277 °C, 280 °C, 285 °C, and 288 °C shows a series of reactions during

the PAN fibers pre-oxidation, including the cyclization, the dehydrogenation, and the oxidation reaction. As mentioned in the introduction section, the conventional MW2D has a difficulty of detecting weak transitions of polymers. So, if we neglect of other transitions, which cannot be detected by DSC or the conventional MW2D, the wrong conclusion about the reaction pathways will probably be summed up, which will be a big problem to mislead people.

We want to find out whether there are other transitions exist during the PAN fibers pre-oxidation. Then, the auto-correlation scaling-MW2D was employed in our work. The scaling-MW2D FTIR spectra of the pre-oxidation of PAN copolymer fibers in the region of 3450–2780 cm^{-1} , 2280–2170 cm^{-1} and 1750–1000 cm^{-1} are shown in **Figure 5**. As expected, using the scaling-MW2D FTIR spectra, not only the strong transition within 277–288 $^{\circ}\text{C}$, but also other weak transitions

are detected when the temperature is below 223 $^{\circ}\text{C}$. Specifically, a weak correlation peak of 1626 cm^{-1} at 100 $^{\circ}\text{C}$ is observed, and the correlation peak of 2243 cm^{-1} within 70–195 $^{\circ}\text{C}$ is detected. The bands at 1626 cm^{-1} is attributed to O–H bending of the absorbed water in PAN fibers,⁴⁸ and 100 $^{\circ}\text{C}$ is exactly the boiling point of water. Thus, this weak transition is certainly the dehydration of PAN fibers. The bands at 2243 cm^{-1} is assigned to C \equiv N stretching.^{10, 13, 15, 17} The weak transition of C \equiv N groups within 70–195 $^{\circ}\text{C}$ indicates some of weak chemical reactions between C \equiv N groups and other functional groups. In our FTIR experiment, it can also be observed that the spectral intensity of 2243 cm^{-1} slowly decreases (not displayed here) with the temperature increasing from 69 $^{\circ}\text{C}$ to 223 $^{\circ}\text{C}$, which also shows the reactions of C \equiv N groups.

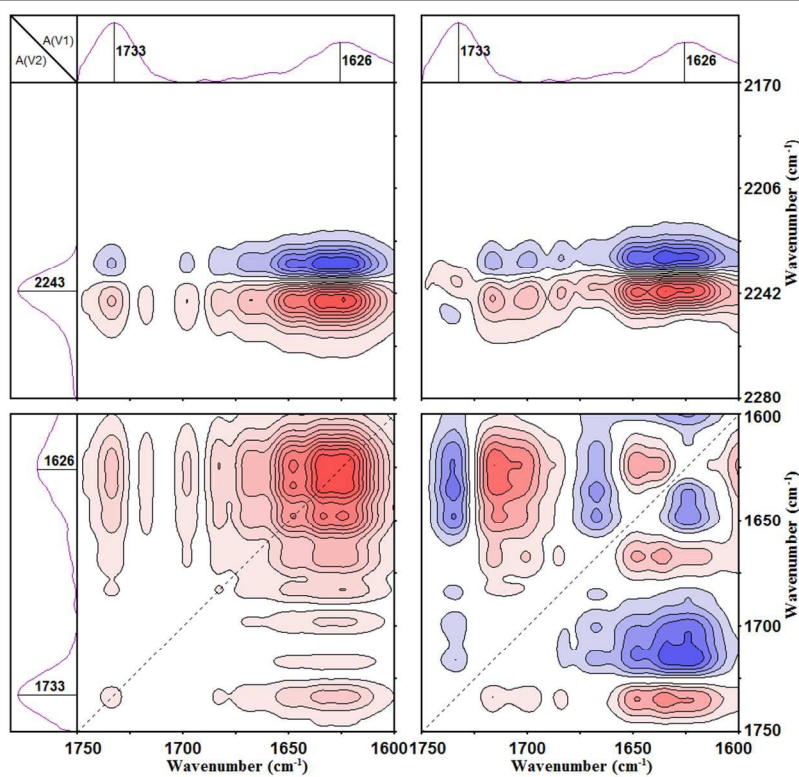


Figure 6. Synchronous (left) and asynchronous (right) correlation FTIR spectra calculated from the *in situ* FTIR spectra of process A (69–223 $^{\circ}\text{C}$) in the region of 1750–1600 cm^{-1} vs 2280–2170 cm^{-1} and 1750–1600 cm^{-1} . Red and blue areas represent the positive and negative correlation intensity, respectively.

From the scaling-MW2D FTIR spectra, two processes of the PAN fibers pre-oxidation are preliminary determined. Here, as shown in **Figure 5**, the temperature point of 223 $^{\circ}\text{C}$ is used as the dividing line between two processes. This is because 223 $^{\circ}\text{C}$ is obviously the onset point of the strong transition judging from the correlation intensity peaks in **Figure 5**. In addition, the temperature of 223 $^{\circ}\text{C}$ is very close to the onset point of 225 $^{\circ}\text{C}$ determined from DSC. As labeled in **Figure 5**, these two processes are named as A and B, and the temperature regions are 69–223 $^{\circ}\text{C}$ and 223–309 $^{\circ}\text{C}$, respectively. According to the strength of the correlation peaks, combining with the DSC curve, it can be inferred that

process B (223–309 $^{\circ}\text{C}$) is the main process of the PAN fibers pre-oxidation, and process A (69–223 $^{\circ}\text{C}$) is the initial process. The cyclization, dehydrogenation, and oxidation of the PAN fibers mainly take place in process B due to the appearance of the strong correlation peaks at 1650 cm^{-1} (C=O, cyclic), 1610 cm^{-1} (C=C, cyclic), 1580 cm^{-1} (C=N, cyclic), 2195 cm^{-1} (C \equiv N, β -amino), and so on. The process B is an exothermic reaction, which can also be easily detected by DSC. The process A is composed of the dehydration of PAN fibers and some of weak reactions of C \equiv N groups. The exothermic and endothermic of these two sub-processes are probably both very weak, and therefore, it cannot be detected using DSC.

Because the formation of the cyclic structures (1650 cm^{-1} , 1610 cm^{-1} , 1580 cm^{-1}) and β -amino nitrile (2195 cm^{-1}) are not observed in process B, we think the weak reactions of $\text{C}\equiv\text{N}$ groups in process B is probably the induced reaction before the rings formation. According to the literature, people generally accepted that comonomer units (e.g., MMA) can significantly reduce the difficulty of PAN ring formation reaction due to the induction. So, it can be inferred that this induced reaction is probably between acrylonitrile (AN) monomer units and MMA. However, in scaling-MW2D, there is no evidence to support our inference about this induced reaction. To solve this problem, the generalized 2D correlation FTIR analysis for process A and B is necessary.

3.5. Generalized 2D correlation FTIR analysis

To capture the detailed pathways of the initial process (A) and the main process (B) during the PAN fibers pre-oxidation, the *in situ* FTIR spectra within process A ($69\text{--}223\text{ }^\circ\text{C}$) and process B ($223\text{--}309\text{ }^\circ\text{C}$) were used to perform the generalized 2D correlation analysis. Generalized 2D correlation FTIR spectra contain synchronous and asynchronous spectra. The sequential order of the spectral intensity change of functional groups can be determined by the sign of the correlation peaks using Noda's rules.²⁴ A simple summarization of Noda's rules is as follows:

- 1) If $\Phi(v_1, v_2) > 0$, $\Psi(v_1, v_2) > 0$ or $\Phi(v_1, v_2) < 0$, $\Psi(v_1, v_2) < 0$, then the movement of v_1 is before that of v_2 ;
- 2) If $\Phi(v_1, v_2) > 0$, $\Psi(v_1, v_2) < 0$ or $\Phi(v_1, v_2) < 0$, $\Psi(v_1, v_2) > 0$, then the movement of v_1 is after that of v_2 ;
- 3) If $\Phi(v_1, v_2) > 0$, $\Psi(v_1, v_2) = 0$ or $\Phi(v_1, v_2) < 0$, $\Psi(v_1, v_2) = 0$, then the movements of v_1 and v_2 are simultaneous.

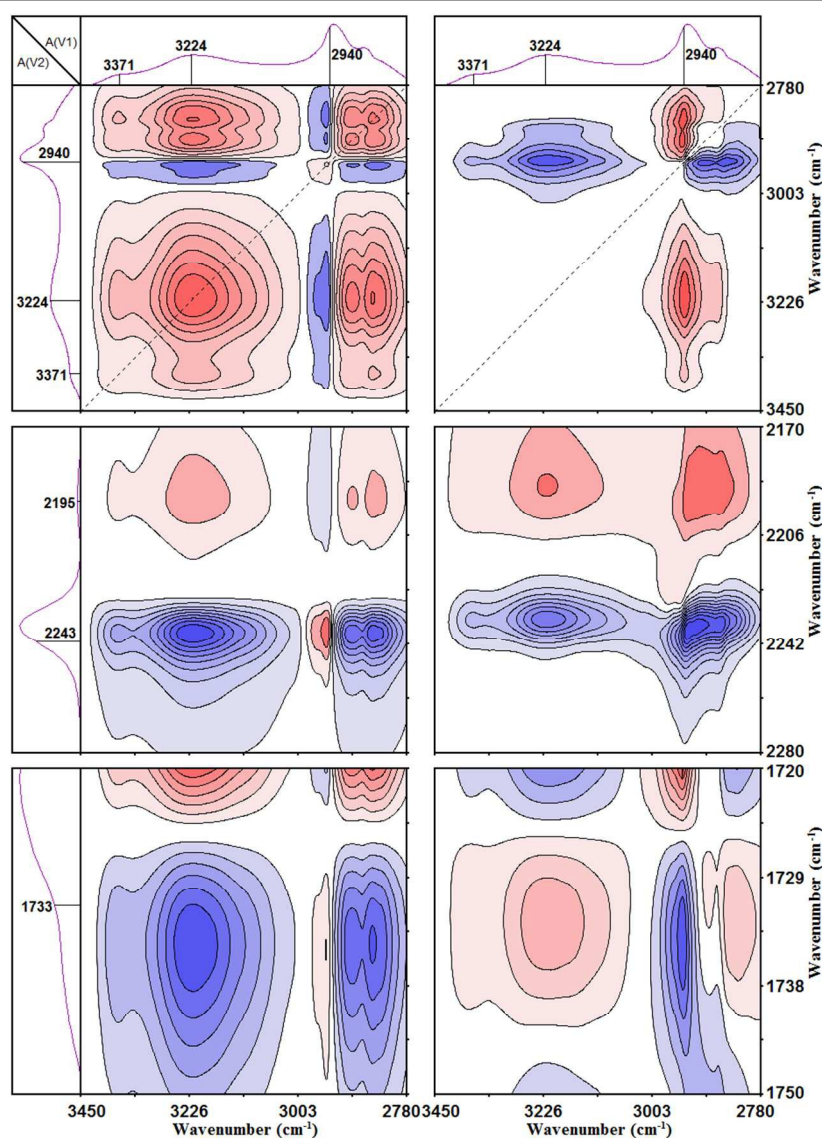


Figure 7. Synchronous (left) and asynchronous (right) correlation FTIR spectra calculated from the *in situ* FTIR spectra of process B ($223\text{--}309\text{ }^\circ\text{C}$) in the region of $3450\text{--}2780\text{ cm}^{-1}$, $3450\text{--}2780\text{ cm}^{-1}$ vs $2280\text{--}2170\text{ cm}^{-1}$, and $3450\text{--}2780\text{ cm}^{-1}$ vs $1750\text{--}1720\text{ cm}^{-1}$.

3.5.1 Initial process of the pre-oxidation (process A, 69–223 °C)

As mentioned above, the process A contains the dehydration of PAN fibers and the induced reaction between AN and MMA. So, we focus the generalized 2D correlation analysis on 1626 cm^{-1} (the absorbed water), 1733 cm^{-1} (MMA), and 2243 cm^{-1} ($\text{C}\equiv\text{N}$). The generalized 2D correlation FTIR spectra in the region $1750\text{--}1600\text{ cm}^{-1}$ vs $2280\text{--}2170\text{ cm}^{-1}$ and $1750\text{--}1600\text{ cm}^{-1}$ are shown in **Figure 6**, which are calculated from the *in situ* spectra of process A (69–223 °C). The signs of the correlation peaks at $(1733\text{ cm}^{-1}, 1626\text{ cm}^{-1})$, $(1733\text{ cm}^{-1}, 2243\text{ cm}^{-1})$, and $(1626\text{ cm}^{-1}, 2243\text{ cm}^{-1})$ are summarized in **Table S3** in the supporting information. The sequential order is gained as $1626\text{ cm}^{-1}\rightarrow 1733\text{ cm}^{-1}\rightarrow 2243\text{ cm}^{-1}$ according to Noda's rules. Here, the symbol " \rightarrow " represents "before", and " \leftarrow " represents "after".

The corresponding sequential order of the groups' movement is $\delta(\text{O-H, absorbed water})\rightarrow\nu(\text{C=O, MMA})\rightarrow\nu(\text{C}\equiv\text{N})$. That is to say, the dehydration of the absorbed water in PAN copolymer fibers is the first step, followed by the movement of C=O groups in MMA units and the movement of C \equiv N groups in AN units. It is noted that the molecular movement of C=O groups in MMA units is before that of C \equiv N groups in AN units. This reveals that the reaction of C \equiv N groups is initiated by the ester groups of MMA, which validates our inference of the induced reaction between MMA and AN units in process A. This result is also the same as the induction period as reported in other literature.^{15, 22} However, the difference of our finding is that the induced reaction between MMA and AN units already takes place at a relatively low temperature (below 223 °C). Comparing with the main process of the PAN fibers pre-oxidation (process B), although process A is very weak, it is very important for PAN cyclization in process B.

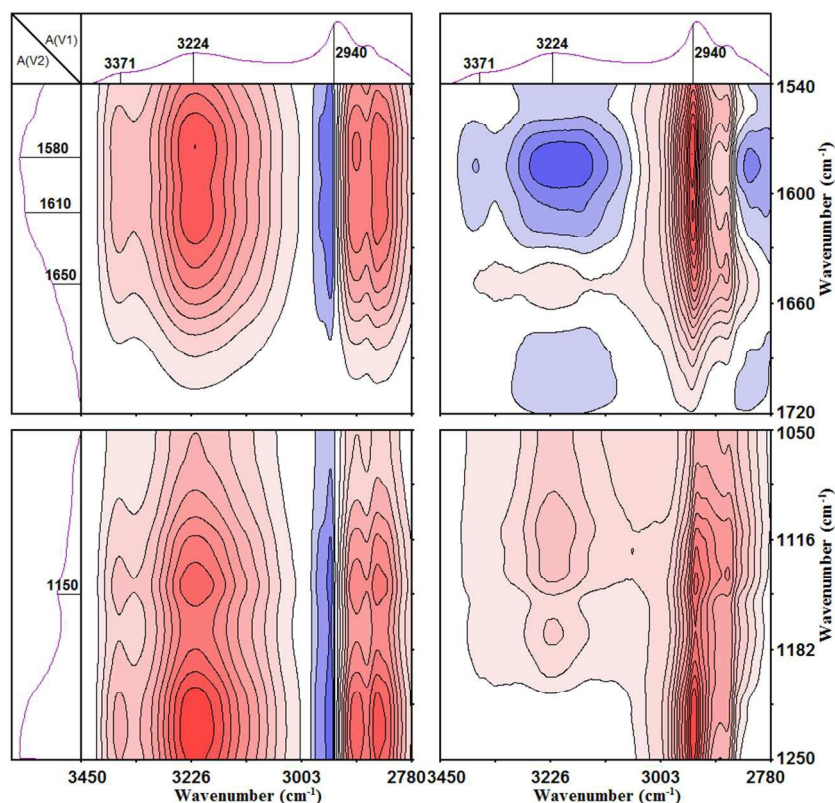


Figure 8. Synchronous (left) and asynchronous (right) correlation FTIR spectra calculated from the *in situ* FTIR spectra of process B (223–309 °C) in the region of $3450\text{--}2780\text{ cm}^{-1}$ vs $1720\text{--}1540\text{ cm}^{-1}$, and $3450\text{--}2780\text{ cm}^{-1}$ vs $1250\text{--}1050\text{ cm}^{-1}$.

3.5.2 Main process of the pre-oxidation (process B, 223–309 °C)

The generalized 2D correlation FTIR spectra calculated from the *in situ* spectra of process B (223–309 °C) are shown in **Figures 7, 8, 9, 10, and 11**. The signs of the correlation peaks of all cross peaks in **Figures 7, 8, 9, 10, and 11** are summarized in **Table S4** in the supporting information. According to Noda's rules, the sequential order is 1733 cm^{-1}

$\rightarrow 1580\text{ cm}^{-1}\rightarrow 1610\text{ cm}^{-1}\rightarrow 3371\text{ cm}^{-1}=3224\text{ cm}^{-1}\rightarrow 1650\text{ cm}^{-1}\rightarrow 1150\text{ cm}^{-1}\rightarrow 2243\text{ cm}^{-1}\rightarrow 2190\text{ cm}^{-1}\rightarrow 2940\text{ cm}^{-1}$.

The corresponding sequential order of the groups' movement is $\nu(\text{C=O, MMA})\rightarrow\nu(\text{C=N, cyclic})\rightarrow\nu(\text{C=C, cyclic})\rightarrow\nu(\text{O-H})=\nu(\text{N-H})\rightarrow\nu(\text{C=O, cyclic})\rightarrow\nu(\text{C-O-C})\rightarrow\nu(\text{C}\equiv\text{N})\rightarrow\nu(\text{C}\equiv\text{N, } \beta\text{-amino})\rightarrow\nu_{as}(-\text{CH}_2-)$. The molecular movement of C=O groups in MMA units is the first of the process B. Then, the movements of C=N and C=C in the cyclic structures are followed. In addition, the movement of

C=N in the cyclic structures is before that of C=C in the cyclic structures. Many scientists reported in FTIR 1580 cm^{-1} (C=N, cyclic) and 1610 cm^{-1} (C=C, cyclic) were the most important characteristics bands for monitoring the formation of PAN cyclic structure.^{15, 42, 43} In our opinion, $\nu(\text{C=O, MMA}) \rightarrow \nu(\text{C=N, cyclic}) \rightarrow \nu(\text{C=C, cyclic})$ actually reveals the generation of some initial cyclic structure in PAN copolymer fibers. The movement of $\nu(\text{C=O, MMA})$ is a natural result of process A, indicating the initial cyclization starting from the

chemical structure formed by the induced reaction between MMA and AN units in the process A. For the initial cyclization, it also shows that the C=N structure is first generated, and then the C=C structure. In order to clear explanation the reaction pathways gained from 2D correlation FTIR analysis, the chemical structures discussed here are all illustrated in **Figure 12**. After that, the oxygen in the air is involved in, and the oxidation reaction occurs. The oxygen attacks the carbon atoms from $-\text{C}=\text{C}-$ structure, and the

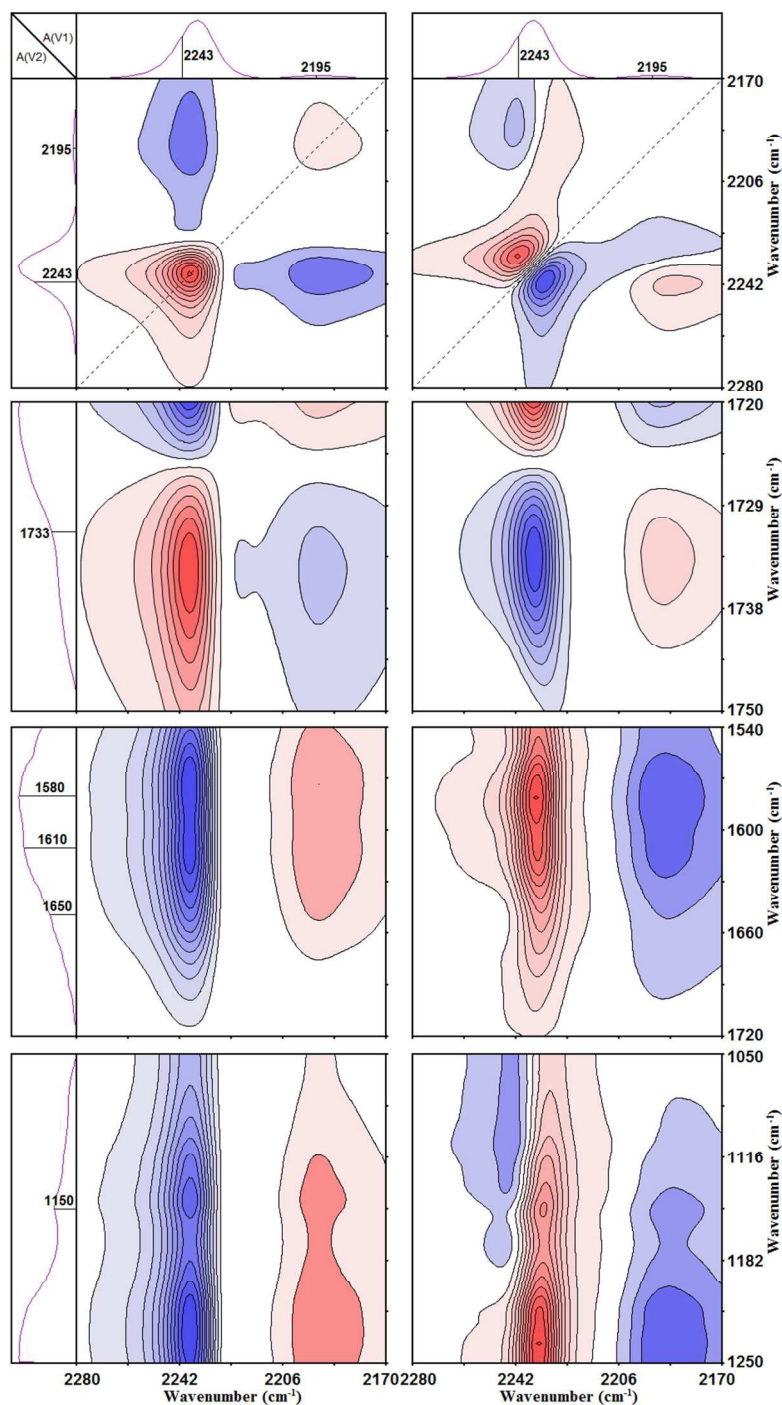


Figure 9. Synchronous (left) and asynchronous (right) correlation FTIR spectra calculated from the *in situ* FTIR spectra of process B (223–309 °C) in the region of $2280\text{--}2170\text{ cm}^{-1}$, $2280\text{--}2170\text{ cm}^{-1}$ vs $1750\text{--}1720\text{ cm}^{-1}$, $2280\text{--}2170\text{ cm}^{-1}$ vs $1720\text{--}1540\text{ cm}^{-1}$, and $2280\text{--}2170\text{ cm}^{-1}$ vs $1250\text{--}1050\text{ cm}^{-1}$.

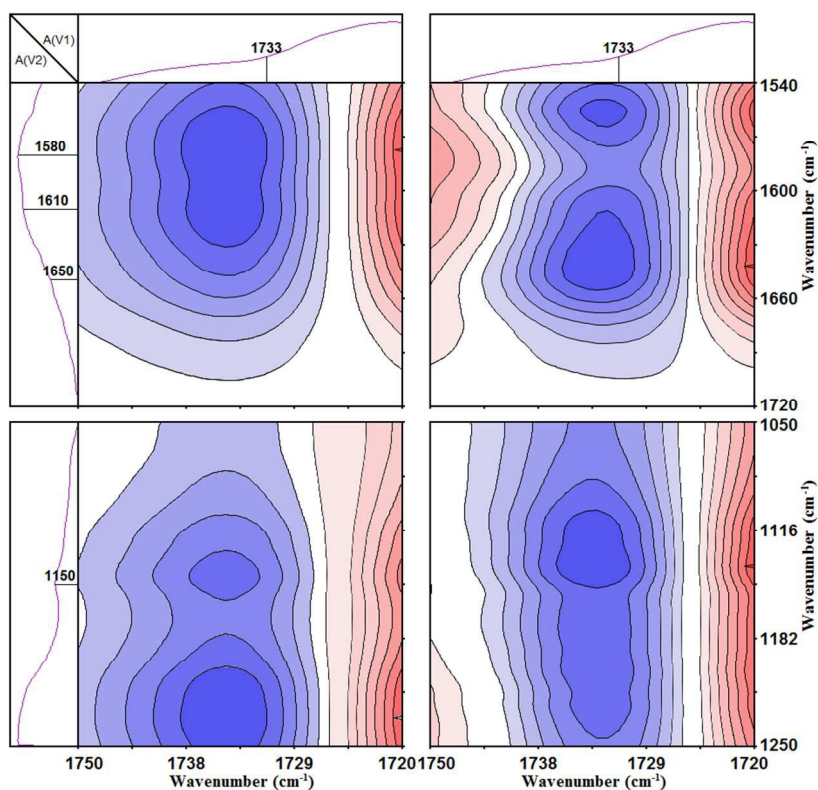


Figure 10. Synchronous (left) and asynchronous (right) correlation FTIR spectra calculated from the *in situ* FTIR spectra of process B (223–309 °C) in the region of 1750–1720 cm^{-1} vs 1720–1540 cm^{-1} and 1750–1720 cm^{-1} vs 1250–1050 cm^{-1} .

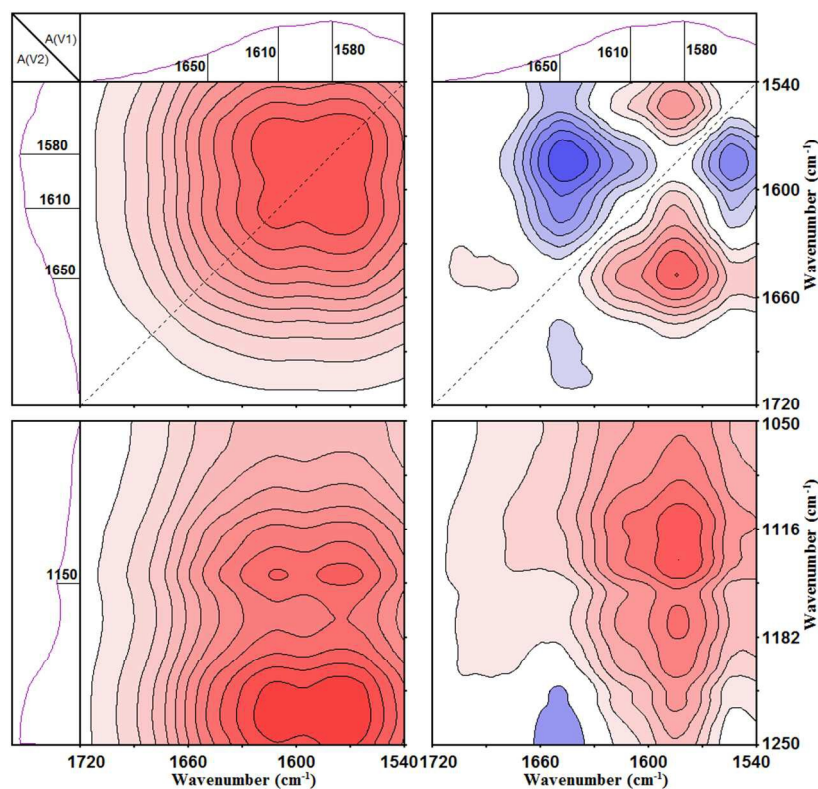


Figure 11. Synchronous (left) and asynchronous (right) correlation FTIR spectra calculated from the *in situ* FTIR spectra of process B (223–309 °C) in the region of 1720–1540 cm^{-1} and 1720–1540 cm^{-1} vs 1250–1050 cm^{-1} .

hydroxyl pyridine structure ($-\text{C}=\text{C}-\text{OH}$) is formed. At the same time, the isomerization of the $\text{C}=\text{N}$ structure is induced. The $\text{N}-\text{H}$ group is formed due to the electrophilic attacking of the active H on the nitrogen atom in $\text{C}=\text{N}$. As everyone knows, the structure of $-\text{C}=\text{C}-\text{OH}$ is unstable, which can be easily transformed into a quasi-pyridone structure with $-\text{C}=\text{O}$. The assumption of the sub-process of $\nu(\text{O}-\text{H})=\nu(\text{N}-\text{H})\rightarrow\nu(\text{C}=\text{O}, \text{cyclic})$ was proposed by other scientists.^{22, 47} In this study, the

assumption is supported by the results of 2D correlation FTIR for the first time. The generation of $\text{C}-\text{O}-\text{C}$ is after that of the quasi-pyridone structure. The $\text{C}-\text{O}-\text{C}$ structure (as shown in **Figure 12**) was also proposed and reported by Standage and Matkowschi.⁴⁹ The main reason of the $\text{C}-\text{O}-\text{C}$ formation is probably due to the dehydration reaction of adjacent hydroxyls on the initial cyclic structure.

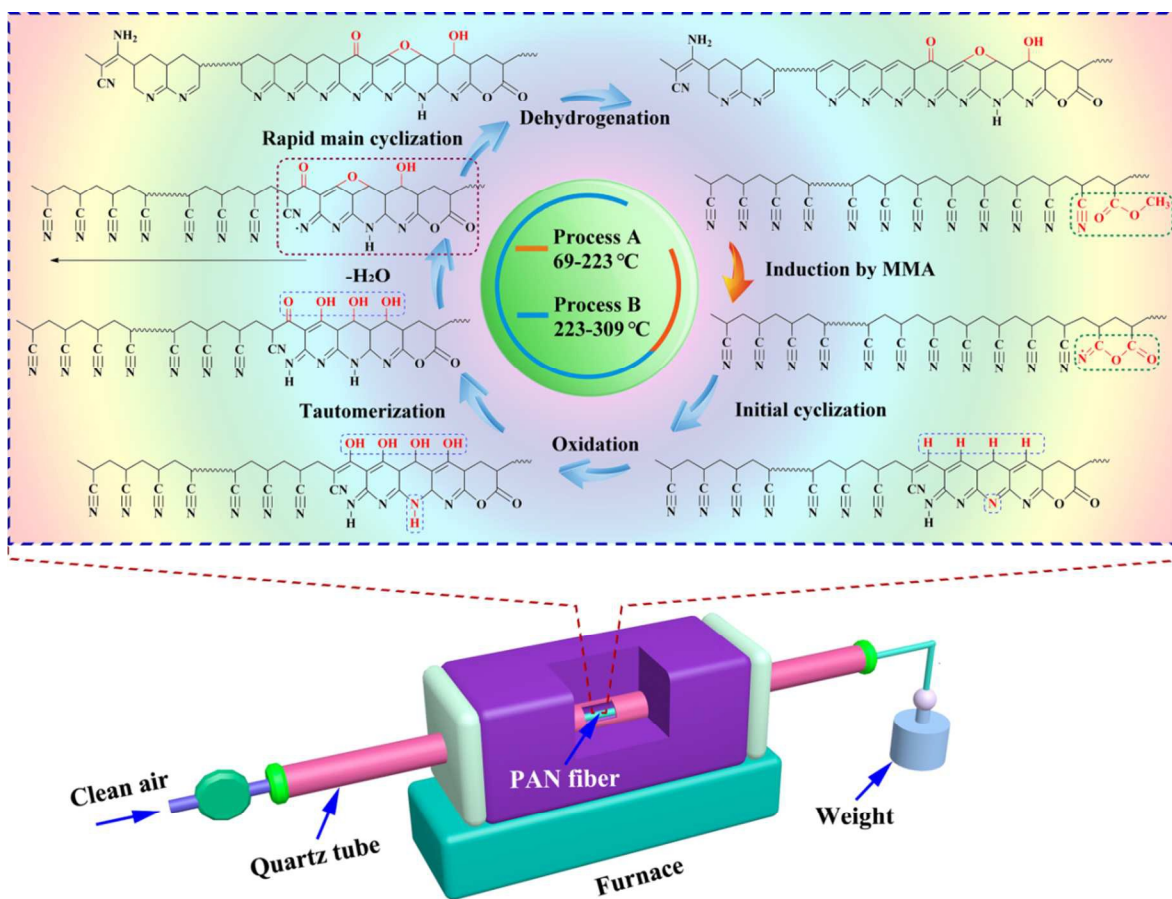


Figure 12. Schematic illustration of the pre-oxidation pathways of PAN copolymer fibers.

According to the sequential order of 2D correlation analysis, after the formation of $\text{C}-\text{O}-\text{C}$, the movement of $\text{C}\equiv\text{N}$ groups appears. In our *in situ* FTIR experiment, the sudden rapid decrease of the bands intensity of $\text{C}\equiv\text{N}$ groups (2243 cm^{-1}) was observed in process B, which indicated the strong chemical reaction of $\text{C}\equiv\text{N}$ groups. The sub-process of $\nu(\text{C}\equiv\text{N})\rightarrow\nu(\text{C}=\text{N}, \beta\text{-amino})$ certainly reveals the main cyclization reaction from a large number of AN units, and then produces some products of β -amino nitriles. In *in situ* FTIR experiment, we also observe the gradual increase of the bands intensity of β -amino nitrile (2195 cm^{-1}) in process B. Many studies reported that the co-monomer in PAN copolymer fibers significantly reduced the difficulty of ring formation reaction due to the induction of the co-monomer units *via* the nucleophilic attack on the carbon atom of an adjacent nitrile group.^{4, 8, 15, 43, 50} However, from the sequential order of 2D correlation analysis, the more detailed pathways are obtained. As discussed in the previous section, the

induced reaction of MMA units on AN units have already been finished in process A ($69\text{--}223\text{ }^\circ\text{C}$). When the temperature increases to process B ($223\text{--}309\text{ }^\circ\text{C}$), the initial cyclic structures are formed from the chemical structure formed by the induced reaction in the process A. Then, these initial cyclic structures undergo a series of the oxidation reactions and the subsequent isomerization reaction and the generation reaction of the $\text{C}-\text{O}-\text{C}$ structure. The initial cyclic structures after the oxidation, the isomerization, and so on are the real induced center and the starting point of the main cyclization reaction. This also reveals that the oxygen in the air plays an important role on the PAN cyclization. The β -amino nitrile is the products of the main cyclization reaction. The appearance of β -amino nitrile in PAN pre-oxidation was also reported by Bajaj et al.⁵¹ and by Gupta et al.⁵² The most likely location of β -amino nitrile is at the end of the polycyclic structure. The last step of the sequential order is the movement of $-\text{CH}_2-$ groups. In *in situ*

FTIR experiment, a rapid reduction of the $-\text{CH}_2-$ bands intensity (2940 cm^{-1}) was observed in process B, especially around $288\text{ }^\circ\text{C}$, also detected by Scaling-MW2D FTIR in **Figure 5**. The concentration reduction of $-\text{CH}_2-$ groups at a high temperature certainly reveals the dehydrogenation reaction on the polycyclic structures.

4. Conclusions

In this study, the *in situ* FTIR spectroscopy combining scaling-MW2D and 2D correlation analysis were used to study the reaction pathways of the PAN copolymer fibers pre-oxidation. Scaling-MW2D revealed that the PAN copolymer fibers pre-oxidation was composed of initial process (process A, $69\text{--}223\text{ }^\circ\text{C}$) and main process (process B, $223\text{--}309\text{ }^\circ\text{C}$). From the sequential order of 2D correlation analysis, the more detailed pathways of PAN fibers pre-oxidation were obtained (**Figure 12**):

1) The induced reaction of MMA units on AN units completed in process A ($69\text{--}223\text{ }^\circ\text{C}$).

2) In process B ($223\text{--}309\text{ }^\circ\text{C}$), the initial cyclic structures were first generated from the chemical structure formed by the induced reaction in process A.

3) Then, these initial cyclic structures underwent a series of the oxidation, the subsequent isomerization, and so on.

4) After that, a large number of AN units were immediately involved in the main cyclization reaction, and some of β -amino nitriles was produced. The initial cyclic structures after the oxidation, the isomerization, and so on were the real induced center of the main cyclization reaction, and therefore, the oxygen in the air played a key role on the PAN main cyclization.

5) The last step was the dehydrogenation reaction on the polycyclic structures at a high temperature.

Acknowledgements

This work was supported by the National Natural Science Foundation of China (Grant Nos. 51473104, 51003066) and State Key Laboratory of Polymer Materials Engineering (Grant No. sklpme2014-3-06, sklpme2014-2-10).

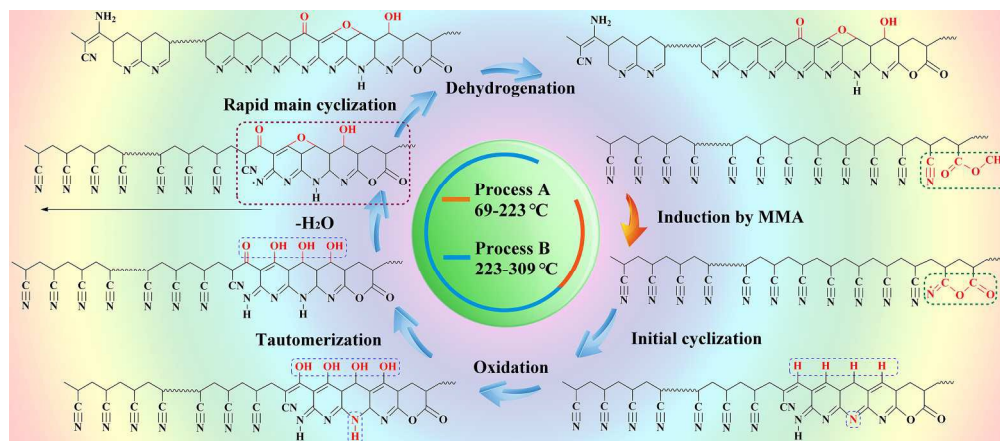
Notes and references

^a State Key Laboratory of Polymer Materials Engineering of China, Polymer Research Institute, Sichuan University, Chengdu 610065, China
*Corresponding author. Tel.: +86-28-85402601; Fax: +86-28-85402465; E-mail address: zhoutaopoly@scu.edu.cn (T. Zhou)

1. Y. Wang, L. Xu, M. Wang, W. Pang and X. Ge, *Macromolecules*, 2014, **47**, 3901-3908.
2. K. Pingkarawat, T. Bhat, D. Craze, C. Wang, R. Varley and A. Mouritz, *Polym. Chem.*, 2013, **4**, 5007-5015.
3. Z. Yang, T. Chen, R. He, H. Li, H. Lin, L. Li, G. Zou, Q. Jia and H. Peng, *Polym. Chem.*, 2013, **4**, 1680-1684.
4. H. Wang, Q. Guo, J. Yang, Z. Liu, Y. Zhao, J. Li, Z. Feng and L. Liu, *Carbon*, 2013, **56**, 296-308.

5. J. Liu, Z. Yue and H. Fong, *Small*, 2009, **5**, 536-542.
6. M. S. A. Rahaman, A. F. Ismail and A. Mustafa, *Polym. Degrad. Stab.*, 2007, **92**, 1421-1432.
7. Y. Zhang, N. Tajaddod, K. Song and M. L. Minus, *Carbon*, 2015, **91**, 479-493.
8. W. X. Zhang, J. Liu and G. Wu, *Carbon*, 2003, **41**, 2805-2812.
9. S.-Y. Kim, S. Lee, S. Park, S. M. Jo, H.-S. Lee and H.-I. Joh, *Carbon*, 2015, **94**, 412-416.
10. T. Usami, T. Itoh, H. Ohtani and S. Tsuge, *Macromolecules*, 1990, **23**, 2460-2465.
11. S. Dalton, F. Heatley and P. M. Budd, *Polymer*, 1999, **40**, 5531-5543.
12. S. H. Bahrami, P. Bajaj and K. Sen, *J. Appl. Polym. Sci.*, 2003, **88**, 685-698.
13. S. C. Martin, J. J. Liggat and C. E. Snape, *Polym. Degrad. Stab.*, 2001, **74**, 407-412.
14. C. Dick, E. Dominguez-Rosado, B. Eling, J. J. Liggat, C. I. Lindsay, S. C. Martin, M. H. Mohammed, G. Seeley and C. E. Snape, *Polymer*, 2001, **42**, 913-923.
15. N.-T. Ngoc Uyen and H. Sung Chul, *Macromolecules*, 2013, **46**, 5882-5889.
16. H. Yang, P. F. Gao, W. B. Wu, X. X. Yang, Q. L. Zeng, C. Li and C. Z. Huang, *Polym. Chem.*, 2014, **5**, 1965-1975.
17. A. Ju, Z. Liu, M. Luo, H. Xu and M. Ge, *J. Polym. Res.*, 2013, **20**, 1-17.
18. Y. Xue, J. Liu, F. Lian and J. Liang, *Polym. Degrad. Stab.*, 2013, **98**, 2259-2267.
19. X. Liu, W. Chen, Y.-I. Hong, S. Yuan, S. Kuroki and T. Miyoshi, *Macromolecules*, 2015, **48**, 5300-5309.
20. S. Soulis and J. Simitzis, *Polym. Int.*, 2005, **54**, 1474-1483.
21. A. F. Thunemann, *Macromolecules*, 2000, **33**, 1790-1795.
22. Y. Xue, J. Liu and J. Liang, *Polym. Degrad. Stab.*, 2013, **98**, 219-229.
23. J. Liu, P. H. Wang and R. Y. Li, *J. Appl. Polym. Sci.*, 1994, **52**, 945-950.
24. I. Noda, *Appl. Spectrosc.*, 1993, **47**, 1329-1336.
25. M. Thomas and H. H. Richardson, *Vib. Spectrosc.*, 2000, **24**, 137-146.
26. S. Morita, H. Shinzawa, I. Noda and Y. Ozaki, *Appl. Spectrosc.*, 2006, **60**, 398-406.
27. S. Morita, K. Kitagawa, I. Noda and Y. Ozaki, *J. Mol. Struct.*, 2008, **883**, 181-186.
28. W. Li and P. Wu, *Polym. Chem.*, 2014, **5**, 5578-5590.
29. W. Li and P. Wu, *Polym. Chem.*, 2014, **5**, 761-770.
30. L. Hou and P. Wu, *RSC Adv.*, 2014, **4**, 39231-39241.
31. T. Zhou, Y. Liu, L. Peng, Y. Zhan, F. Liu, A. Zhang and L. Li, *Anal. Bioanal. Chem.*, 2014, **406**, 4157-4172.
32. Q. Yuan, T. Zhou, L. Li, J. Zhang, X. Liu, X. Ke and A. Zhang, *RSC Adv.*, 2015, **5**, 31153-31165.
33. Y. Liu, W. Li, L. Hou and P. Wu, *RSC Adv.*, 2014, **4**, 24263-24271.
34. T. Zhou, A. Zhang, C. Zhao, H. Liang, Z. Wu and J. Xia, *Macromolecules*, 2007, **40**, 9009-9017.
35. H. Lai and P. Wu, *Polymer*, 2010, **51**, 1404-1412.
36. X. Liu, T. Zhou, Y. Liu, A. Zhang, C. Yuan and W. Zhang, *RSC Adv.*, 2015, **5**, 10231-10242.
37. H. G. Chae, M. L. Minus, A. Rasheed and S. Kumar, *Polymer*, 2007, **48**, 3781-3789.
38. L. Yaodong, C. Han Gi and S. Kumar, *Carbon*, 2011, **49**, 4466-4476.

39. K. L. Gallaher, D. Lukco and J. G. Grasselli, *Canadian Journal of Chemistry-Revue Canadienne De Chimie.*, 1985, **63**, 1960-1966.
40. N. Grassie and R. McGuchan, *Eur. Polym. J.*, 1971, **7**, 1357-1371.
41. S. Deki, H. Nabika, K. Akamatsu, M. Mizuhata, A. Kajinami, S. Tomita, M. Fujii and S. Hayashi, *Thin Solid Films*, 2002, **408**, 59-63.
42. N. Grassie and R. McGuchan, *Eur. Polym. J.*, 1972, **8**, 257-269.
43. H. Kakida, K. Tashiro and M. Kobayashi, *Polym. J.*, 1996, **28**, 30-34.
44. J. Mittal, O. P. Bahl, R. B. Mathur and N. K. Sandle, *Carbon*, 1994, **32**, 1133-1136.
45. H. Kono, S. Yunoki, T. Shikano, M. Fujiwara, T. Erata and M. Takai, *J. Am. Chem. Soc.*, 2002, **124**, 7506-7511.
46. E. Pretsch, P. Bühlmann, C. Affolter, E. Pretsch, P. Bühlmann and C. Affolter, *Structure determination of organic compounds*, Springer, 2009.
47. Z. Fu, Y. Gui, C. Cao, B. Liu, C. Zhou and H. Zhang, *J. Mater. Sci.*, 2014, **49**, 2864-2874.
48. M. Liu, P. Wu, Y. Ding, G. Chen and S. Li, *Macromolecules*, 2002, **35**, 5500-5507.
49. A. Standage and R. Matkowsky, *Eur. Polym. J.*, 1971, **7**, 775-783.
50. I. Karacan and G. Erdogan, *Fibers Polym.*, 2012, **13**, 329-338.
51. P. Bajaj, D. Paliwal and A. Gupta, *J. Appl. Polym. Sci.*, 1993, **49**, 823-833.
52. A. Gupta, D. Paliwal and P. Bajaj, *J. Macromol. Sci. Part C: Polym. Rev.*, 1991, **31**, 1-89.



814x353mm (72 x 72 DPI)